ORIGINAL ARTICLE

MEK–ERK pathway regulates EZH2 overexpression in association with aggressive breast cancer subtypes

S Fujii[1], K Tokita[1], N Wada[2], K Ito[3], C Yamauchi[1], Y Ito[4] and A Ochiai[1]

[1]Pathology Division, Research Center for Innovative Oncology, National Cancer Center at Kashiwa, Kashiwa, Chiba, Japan; [2]Breast Surgery Division, National Cancer Center Hospital East, Kashiwa, Chiba, Japan; [3]Graduate School of Biomedical Sciences, Nagasaki University, Nagasaki, Japan and [4]Cancer Science Institute of Singapore, Proteos, Singapore

EZH2 overexpression occurs in various malignancies and is associated with a poor outcome. We have so far demonstrated that EZH2 downregulates the important genes such as *E-cadherin* and *RUNX3* by increasing histone H3K27 trimethylation. However, the mechanism of EZH2 overexpression in various cancer cells remains unclear. In this study we carried out a promoter analysis of the *EZH2* gene and investigated whether a survival signal that is upregulated in cancer cells is related to overexpression at the transcription level. We also explored the clinical relevance of the signaling pathway that leads to EZH2 overexpression in breast cancer and demonstrated that MEK–ERK1/2–Elk–1 pathway leads to EZH2 overexpression. The triple-negative and ERBB2-overexpressing subtypes of breast cancer are known to contain more rapidly proliferating breast cancer cells. The signaling pathway connected to EZH2 overexpression was associated with both aggressive subtypes of breast cancer. We show the significance that overexpression of histone modifier protein EZH2 in cancer cells and our study could pave the way for EZH2 inhibition to become an efficient treatment for more aggressive breast cancers.
Oncogene (2011) **30**, 4118–4128; doi:10.1038/onc.2011.118; published online 18 April 2011

Introduction

Enhancer of zeste homolog 2 (EZH2) is well known to be a histone modifier protein that functions as a methytransferase at lysine 27 of histone H3 (Cao *et al*., 2002). EZH2 is also a member of the polycomb group of proteins and belongs to the polycomb repressive complex 2 (PRC2) subgroup (Schuettengruber *et al*., 2007), and EZH2 has an important role in X-chromo-some inactivation (Plath *et al*., 2003). On the other hand, there have been several reports that overexpression of EZH2 occurs in various malignancies and that it is associated with a poor outcome in prostate cancer and breast cancer (Varambally *et al*., 2002; Kleer *et al*., 2003). In an attempt to determine the functional role of EZH2 overexpression in cancer tissue, we have already demonstrated that EZH2 downregulates important genes, such as *E-cadherin* and *RUNX3*, by increasing histone H3K27 trimethylation, which suggests that it may be an oncogene (Fujii *et al*., 2008; Fujii and Ochiai, 2008). However, the mechanism of EZH2 overexpression in various cancer cells remains unclear. Although overexpression of EZH2 protein detected by immunohistochemical staining in various clinical tissue samples is associated with a poor outcome (Bachmann *et al*., 2006), the mechanism responsible for the differences in rates of cancer cell positivity between individual cases also remains unclear.

Breast cancer is a heterogeneous disease with respect to outcome and response to treatment. The clinical course and treatment of breast cancer patients are to a large extent driven by the biological characteristics of their tumors, and accurate classification of breast cancers is of major importance. Expression of estrogen receptor (ER) or progesterone receptor (PgR) and epidermal growth factor receptor 2 (ERBB2) identified by immunohistochemical staining has long guided the classification of breast cancer, and the classification has proved useful in terms of predicting outcome and guiding treatment recommendations. Hormone receptor- (ER or PgR) positive breast cancers and ERBB2-positive breast cancers currently account for 75–80% and 15–20%, respectively, of all breast cancers. About half of ERBB2-positive cancers co-express hormone receptors (Slamon *et al*., 1989; Konecny *et al*., 2003), and the other 10–15% of breast cancers fall into the so-called triple-negative category, defined by the absence of expression of all three proteins. As a result, triple-negative breast cancers are resistant to existing targeted therapies, namely, trastuzumab and hormonal therapies. The pathways that drive proliferation of triple-negative breast cancer cells are still poorly understood. Five distinct subtypes of breast cancer, that is, a luminal subtype A, a luminal subtype B, an ERBB2-overexpressing subtype, a basal subtype and a normal

Correspondence: Dr A Ochiai, Pathology Division, Research Center for Innovative Oncology National Cancer Center at Kashiwa, 6-5-1, Kashiwanoha, Kashiwa, Chiba 277-8577, Japan.
E-mail: aochiai@east.ncc.go.jp

breast-like subtype have been defined by RNA expression arrays (Perou et al., 2000), and this classification has been refined by cytokeratin (CK) expression patterns. Although most basal-type breast cancers do not express ER, PgR or ERBB2 (Nielsen et al., 2004), as a small number do, the overlap between basal-type breast cancer and triple-negative breast cancer is not complete. However, characteristically these tumors have a high mitotic count, scant stromal content, exhibit central necrosis, a pushing border of invasion, frequent apoptotic cells and a stromal lymphocytic response. The classification of breast cancers is clinically relevant because a higher proportion of patients with basal-type breast cancer have a poor outcome than patients with luminal type-breast cancer (Korsching et al., 2008).

Previous studies have shown that increased expression of EZH2 is associated with aggressive behavior of breast cancers and a high breast cancer cell proliferation rate (Kleer et al., 2003; Bachmann et al., 2006). In this study we carried out a promoter analysis of the EZH2 gene and investigated whether a survival signal that is upregulated in cancer cells is related to overexpression at the transcription level. We also explored the clinical relevance of the signaling pathway that leads to EZH2 overexpression in breast cancer.

Results

Promoter analysis

The -2874 to $+599$ (transcription start site designated as $+1$) long 5′ flanking region of EZH2 was obtained by PCR amplification of human placenta genomic DNA. The fragment was then subcloned into the promoter-less luciferase reporter vector pGL3-Basic, and the putative promoter activity was measured by a dual-luciferase assay (Figure 1a). pGL3-Basic had basal strength in the form of luc $+$/Rluc activity, and that strength was set equal to 1. The deletion variants of the EZH2 promoter region yielded different basal levels of expression of the luciferase gene. One of them, pGL3-696 exhibited about twofold increase in relative luciferase activity in
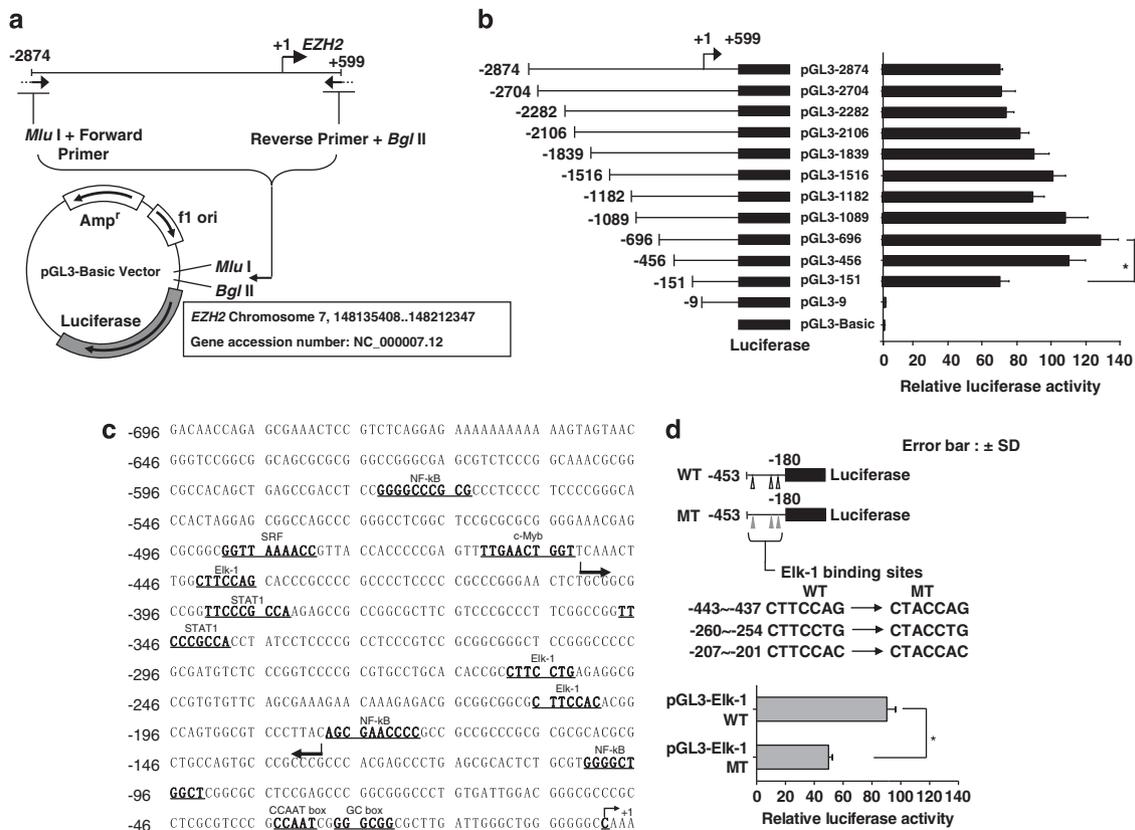

Figure 1 Promoter analysis of the EZH2 promoter. (**a**) Construction of reporter plasmids with the EZH2 promoter region and deletion variants inserted. The gene accession number is NC_000007.12. The reporter plasmid pGL3-2874 was constructed by inserting the PCR product of the putative EZH2 promoter region into the MCS between the MluI and BglII sites of pGL3-Basic. $+1$ means the transcriptional start site. (**b**) Deletion variants of the EZH2 promoter pGL3-2704, 2282, 2106, 1839, 1516, 1182, 1089, 696, 456 and 151 were derived from pGL3-2874. Asterisk mark focuses a difference of relative luciferase activity between pGL3-696 and pGL3-151 constructs. (**c**) Bioinformatic analysis of transcriptional factor binding sites in the EZH2 5′-flanking upstream region. Software was used to make the predictions. The numbers on the left side indicate the order upstream to the first base of the transcriptional start site. The transcription factors that bind to the region are labeled below their corresponding binding sites. The DNA sequence surrounded by two arrows was for mutation construct. (**d**) Three Elk-1 binding motifs were located within -453 nt and -180 nt. White and gray triangles indicate a wild or mutant sequence for Elk-1 binding motifs, respectively. WT, wild type; MT, mutant type.

comparison with that of pGL3-2874, and its activity was higher than that of the full-length promoter (pGL3-2874) (Figure 1b). A significant difference in relative luciferase activity between pGL3-696 and pGL3-151 was exhibited as about twofold difference between the deletion variants ($P < 0.05$), and pGL3-151 displayed much lower relative luciferase activity than pGL3-696. We focused on the region responsible for the difference in relative luciferase activity and carried out a computational analysis with the TRANSFAC 6.0 software program (BIOBASE, Beverly, MA, USA; http://www.biobase-international.com/pages/index.php?id = transfac). The results revealed the expected enhancer sequences, such as CCAAT box and GC box, as well as transcription factor-binding sites. Within the −696 nt of the *EZH2* 5′ flanking region, there were three Elk-1 binding motifs, as well as many general transcription factors that constitute the basal transcription apparatus and response elements, including NF-κB, c-Myb, STAT1 and SRF (serum response factor), which is known to cooperate with Elk-1 for transcriptional activation (Figure 1c). There were three binding sites of Elk-1 between −696 nt and –151 nt of the *EZH2* 5′ flanking region (Figure 1d), suggesting that the MEK–ERK–Elk-1 pathway, which is known to be upregulated in various cancer cells, contributes to the EZH2 overexpression. Next, we made wild and mutant constructs with one point mutation for each Elk-1 binding sites. At first,

wild and mutant DNA sequences of the *EZH2* promoter region encompassing the all three Elk-1 binding sites (the length is 274 bp) were synthesized, respectively, and inserted into pGL3-Basic Vector. Theafter, dual luciferase assays were carried out. The pGL3–Elk-1–MT exhibited almost a half decrease in relative luciferase activity compared with that of wild-type construct (Figure 1d). The decreased level was similar to the difference between deletion construct without three Elk-1 binding sites (pGL3-151) and pGL3–696 construct.

Effect of inhibition of the MEK–ERK–Elk-1 pathway on EZH2 expression

We proceeded to investigate whether inhibition of the MEK–ERK–Elk-1 pathway would affect EZH2 over-expression. First, the cytotoxic effect of the MEK inhibitor (U0126) on MDA-MB-231 cells was assessed by analyzing the cell growth curve. The results showed that the 40 μm concentration of the MEK inhibitor did not significantly affect cell survival, but as a higher concentration (400 μM) caused significant cell death, 40 μM was chosen as the optimal concentration to use in all experiments on MDA-MB-231 cells. The MDA-MB-231 cells were treated with 10 and 40 μM concentrations of the MEK inhibitor for 12 and 24 h, *EZH2* mRNA expression started to decrease at 12, and at 24 h it had reached one-third the level in the control (Figure 2a).
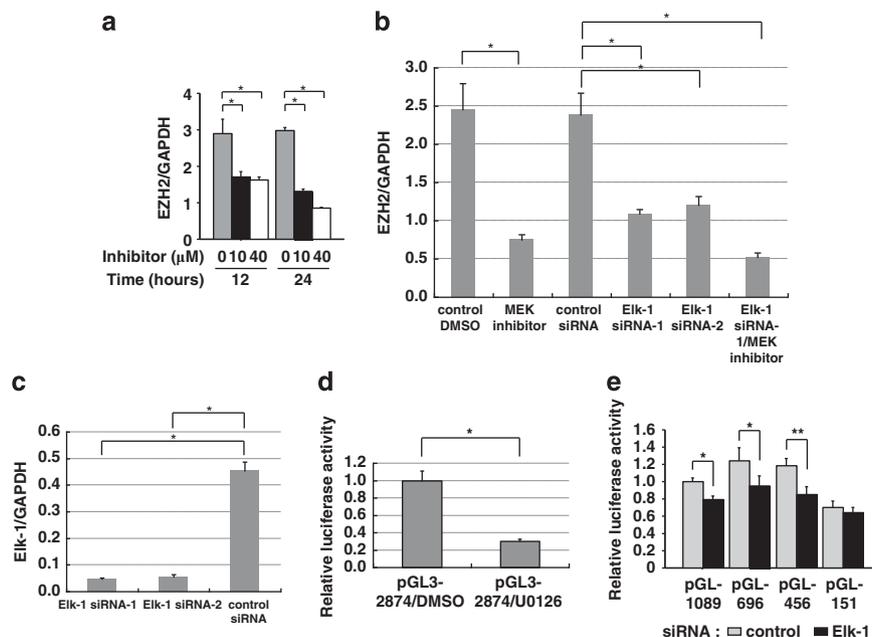

Figure 2 *EZH2* mRNA expression decreased after MEK inhibitor treatment and knockdown of Elk-1 in breast cancer cell line MDA-MB-231. (**a**) *EZH2* mRNA decreased after MEK inhibitor treatment (10 and 40 μM) at 12 and 24 h. (**b**) The level of *EZH2* mRNA decreased after MEK inhibitor treatment and knockdown by *Elk-1* siRNA transfection, and it decreased after a combination of MEK inhibitor treatment and *Elk-1* siRNA transfection. Two kinds of Elk-1 siRNAs (Elk-1 siRNA-1 and Elk-1 siRNA-2) were used to confirm the results. The *EZH2* mRNA expression levels were quantified by real-time RT–PCR. (**c**) The level of *Elk-1* after knockdown by siRNA transfection was also quantified by real-time RT–PCR. (**d**) After the transfection of pGL3-2874 constructed reporter plasmid and addition of MEK inhibitor at a concentration of 40 μM, MDA-MB-231 cells were incubated for 24 h and the reporter assays were carried out. (**e**) After the transfection of *Elk-1* siRNA, MDA-MB-231 cells were incubated for 24 h. Thereafter, four kinds of constructed reporter plasmids were transfected and incubated for 24 h, and the reporter assays were carried out. The results of the real-time RT–PCR and relative luciferase activity are shown in the form of diagrams and the results were statistical analyses by Student's *t* test. *Indicates $P < 0.05$, ** indicates $P < 0.01$, and all data are means + s.d. of data from at least three experiments.

Knockdown of *Elk-1*, the functional transcription factor present in the downstream of the MEK–ERK pathway, by small interfering RNA (siRNA) transfection caused a decrease in level of *EZH2* mRNA expression that was similar to the decrease caused by MEK inhibitor treatment (Figure 2b). A combination of MEK inhibitor treatment and *Elk-1* siRNA transfection resulted in a decrease in level of *EZH2* mRNA expression that was almost the same as in response to treatment with the MEK inhibitor or *Elk-1* siRNA transfection alone (Figure 2b). The efficiency of *Elk-1* knockdown by siRNA transfection is shown in Figure 2c. We tested whether the MEK inhibitor treatment or *Elk-1* knockdown by siRNA transfection affected the relative luciferase activity of *EZH2* promoter. Both treatments affected the relative luciferase activity of *EZH2* promoter. However, in case that pGL3–151 constructed reporter plasmids without predicted Elk-1 binding sites was transfected, the relative

luciferase activity of *EZH2* promoter was not affected by *Elk-1* knockdown (Figure 2e).

Phospho-Elk-1 binds to the promoter of EZH2

Computational analysis identified three Elk-1 binding sites within −696 nt of the *EZH2* 5′-flanking region (Figure 1c). We designed the three sets of PCR primers for the chromatin immunoprecipitation (ChIP) assay so that the amplified region would include or would not include Elk-1 binding sites (Figure 3a). We carried out the ChIP assay to determine whether phospho-Elk-1 or generic Elk-1 binds to a region of *EZH2* gene (Figure 3a). After treatment with the MEK inhibitor, the level of phospho-Elk-1 binding to the promoter region of the *EZH2* gene decreased significantly in comparison with the control ($P < 0.05$) (Figures 3b and c), and it also decreased significantly in comparison with
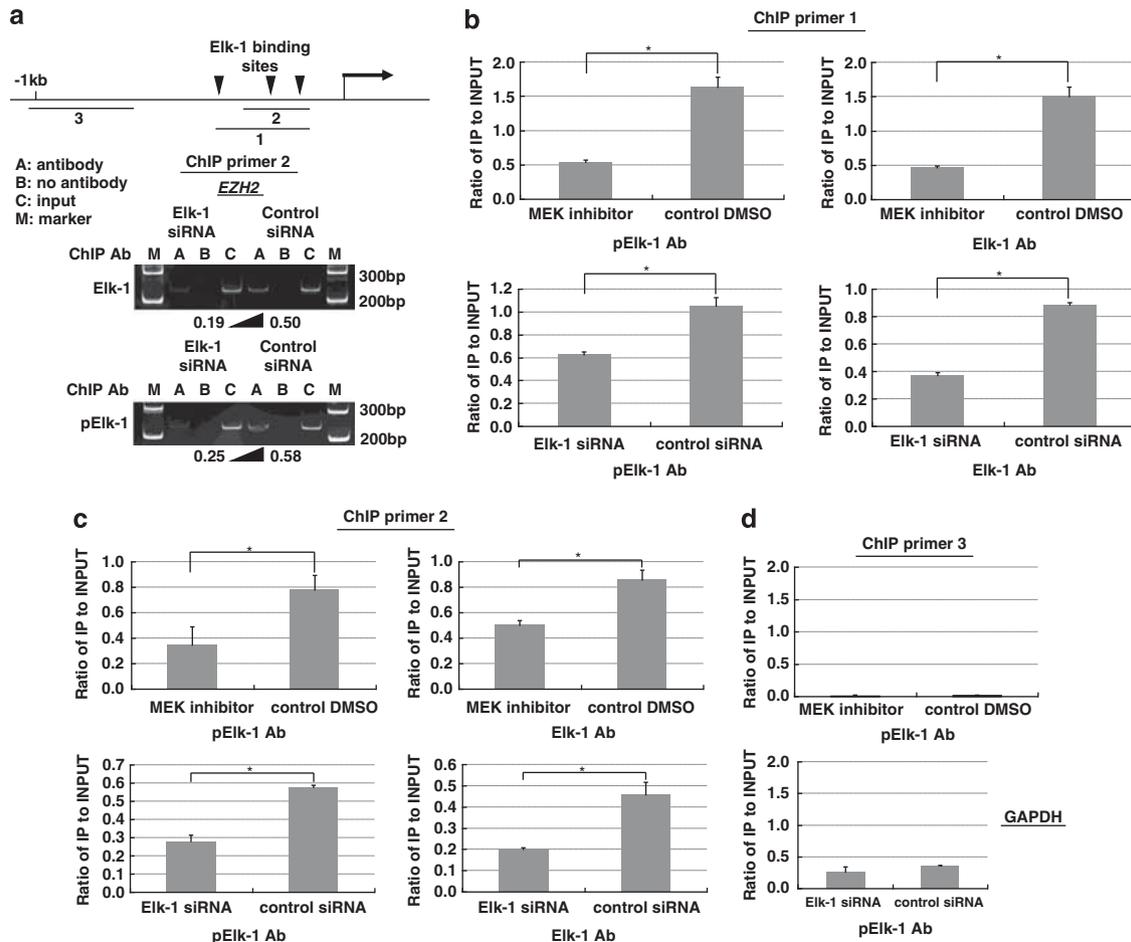

Figure 3 The decrease in *EZH2* mRNA expression after MEK inhibitor treatment and *Elk-1* knockdown was accompanied by a decreased level of phospho-Elk-1 binding to the *EZH2* promoter. (**a**) The three sets of primers for the ChIP assay were designed to encompass Elk-1 binding motif sites or not to encompass Elk-1 binding motif sites. The representative electrophoretic figures on 6%-acrylamide gel were shown and nonspecific immunoprecipitation was excluded. (**b**) ChIP primer 1. (**c**) ChIP primer 2. (**d**) ChIP primer 3 and ChIP primer for *GAPDH gene promoter*. ChIP assay was performed by using DNA–protein complex isolated from MDA-MB-231 cells treated with the MEK inhibitor for 24 h or transfected with *Elk-1* siRNA for 48 h, and immunoprecipitated with phospho-Elk-1 (pElk-1) or generic Elk-1 (Elk-1) antibody. The ratio of immunoprecipitated DNA to input DNA was quantified by performing a DNA 1000 assay with the Agilent 2100 bioanalyzer. Individual ChIP assays were carried out a total of at least three times to confirm the reproducibility of the PCR-based experiment. The results of the ChIP assays are shown in the form of diagrams and statistical analyses by Student's *t* test. *Indicates $P < 0.05$, and all data are means + s.d. of data from at least three experiments.

the control after *Elk-1* siRNA transfection ($P<0.05$) (Figures 3b and c). The binding level of Elk-1 to the EZH2 promoter that was detected using a generic anti-Elk-1 antibody also decreased after MEK inhibitor treatment or Elk-1 knockdown (Figures 3b and c), which suggests that the generic anti-Elk-1 antibody used here recognizes phosphorylated Elk-1, as well as non-phosphorylated Elk-1. On the other hand, it was so difficult to detect signal intensity reflecting binding levels of phospho-Elk-1 to the *EZH2* promoter region without any predicted Elk-1 binding motif and to the non-targeted gene such as *GAPDH* by PCR-based method (Figure 3d). These results suggest that the level of phospho-Elk-1 binding to the *EZH2* promoter region with the predicted Elk-1 binding sites regulates the transcription of *EZH2* mRNA.

MEK–ERK–Elk-1 pathway regulates EZH2 protein expression in triple-negative and ERBB2-overexpressing breast cancer cell lines
The findings described thus far demonstrated the existence of MEK–ERK–Elk-1 pathway that functions

as a regulator of *EZH2* mRNA overexpression in triple-negative breast cancer MDA-MB-231. In the next step, we investigated whether the pathway has a role in regulating EZH2 protein expression in the three different types of breast cancer cell lines, that is, the triple-negative/basal-type (MDA-MB-231 and MDA-MB-468), ERBB2 overexpressing/luminal B type (SKBr3), and hormone receptor-positive type (HCC1500). As shown in Figure 4a, the western blot analysis showed that MEK inhibitor (U0126) treatment decreased EZH2 protein expression in MDA-MB-231 cells. The decrease of EZH2 protein started 4 h after U0126 treatment and it was accompanied by a disappearance of phosphorylation of Elk-1. The decrease of EZH2 protein after U0126 treatment for 12 h was accompanied by a decrease in phosphorylation of both ERK1/2 and Elk-1 (Figure 4b). Knockdown of Elk-1 by siRNA transfection also decreased EZH2 protein expression and decreased Elk-1 of phosphorylation, without decreasing the phosphorylation level of pERK1/2, because Elk-1 is a downstream protein of the MEK–ERK1/2 pathway (Figure 4c). These results were the same as obtained in regard to *EZH2* mRNA after MEK
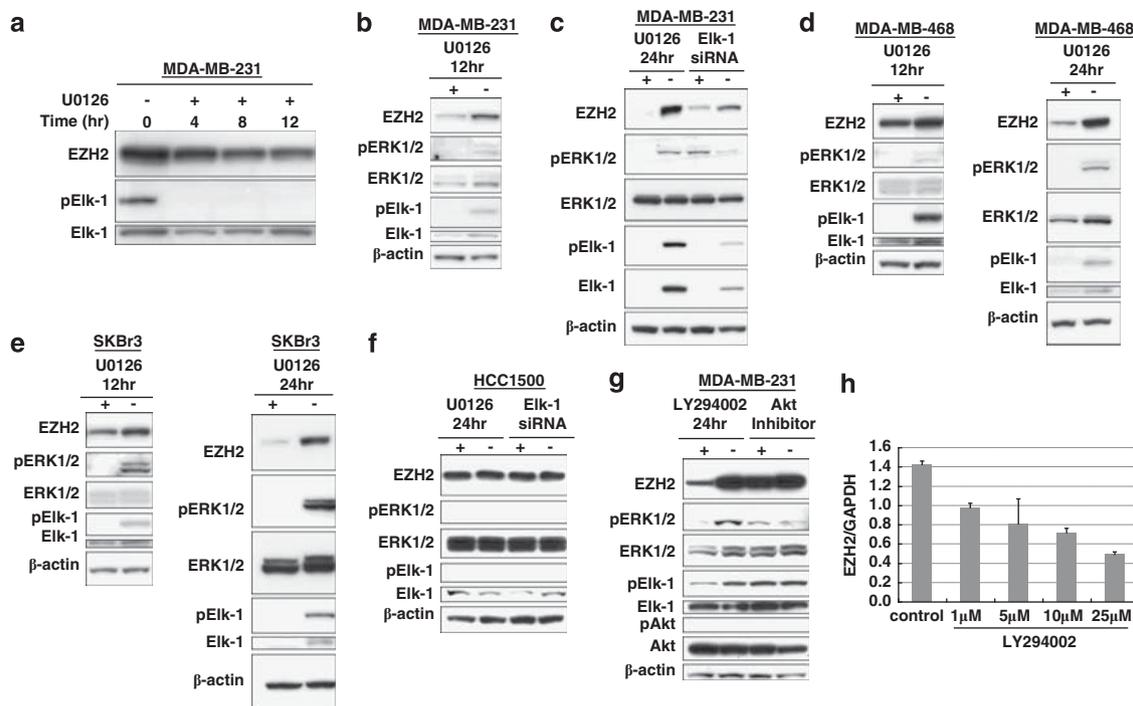

Figure 4 EZH2 protein expression after MEK inhibitor treatment and *Elk-1* siRNA transfection in triple-negative, ERBB2-overexpressing, hormone receptor-positive breast cancer cell lines assessed by western blot analysis. (**a**) Effects of U0126 treatment for 4, 8 and 12 h on Elk-1 phosphorylation, Elk-1 and EZH2 in MDA-MB-231 cells (triple-negative). (**b**) Effects of U0126 treatment for 12 h on EZH2, ERK1/2 phosphorylation, ERK1/2, Elk-1 phosphorylation and Elk-1 in MDA-MB-231 cells. (**c**) Effects of U0126 treatment and Elk-1 knockdown on EZH2, ERK1/2 phosphorylation, ERK1/2, Elk-1 phosphorylation and Elk-1 in MDA-MB-231 cells. Protein was extracted 24 h after MEK inhibitor treatment and 48 h after *Elk-1* siRNA transfection. (**d**) Effects of U0126 treatment for 12 and 24 h on EZH2, ERK1/2 phosphorylation, ERK1/2, Elk-1 phosphorylation and Elk-1 in MDA-MB-468 cells (triple-negative). (**e**) Effects of U0126 treatment for 12 and 24 h on EZH2, ERK1/2 phosphorylation, ERK1/2, Elk-1 phosphorylation and Elk-1 in SKBr3 cells (ERBB2-overexpressing). (**f**) Effects of U0126 treatment and Elk-1 knockdown on EZH2, ERK1/2 phosphorylation, ERK1/2, Elk-1 phosphorylation and Elk-1 in HCC1500 cells (hormone receptor-positive). Protein was extracted 24 h after MEK inhibitor treatment and 48 h after *Elk-1* siRNA transfection. (**g**) Effects of LY294002 (10 μM) or Akt inhibitor (20 μM) treatment on EZH2, ERK1/2 phosphorylation, ERK1/2, Elk-1 phosphorylation, Elk-1, Akt phosphorylation and Akt in MDA-MB-231 cells. Protein was extracted 24 h after MEK inhibitor treatment and 48 h after *Elk-1* siRNA transfection. (**h**) *EZH2* mRNA decreased after PI3K inhibitor treatment (1, 5, 10 and 25 μM) at 24 h in MDA-MB-231 cells.

inhibitor treatment and *Elk-1* siRNA transfection (Figure 2). MEK inhibitor treatment for 12 or 24 h decreased EZH2 protein expression in MDA-MB-468 cells and SKBr3 cells, and the decrease was also accompanied by a decrease in phosphorylation of both ERK1/2 and Elk-1 (Figures 4d and e), results that were similar to those observed in MDA-MB-231 cells. On the other hand, U0126 treatment or *Elk-1* knockdown by siRNA transfection did not have any effect on EZH2 expression in HCC1500 cells (Figure 4f). Next, we treated MDA-MB-231 cells with Akt inhibitor or PI3K inhibitor to determine the specificity of MEK inhibitor with respect to EZH2 expression. AKT inhibitor did not affect EZH2 expression, phospho-AKT was not detected in MDA-MB-231 cells by western blot analysis (Figure 4g), which was same as previous published data (Kenny *et al.*, 2007). *EZH2* mRNA expression also did not change after treatment with Akt inhibitor (Supplementary Figure 1). PI3K inhibitor (LY294002) did affect negatively EZH2 expression. PI3K inhibitor decreased the phosphorylation level of ERK1/2 and Elk-1 (Figure 4g), however, the decrease was not remarkable. The result of real-time reverse-transcription PCR (RT–PCR) showed that PI3K inhibitor decreased *EZH2* mRNA expression level (Figure 4h). These results suggest that PI3K inhibitor affect EZH2 expression negatively by downregulating MEK–ERK–Elk-1 pathway. The previous report shows that Rac exerts an effect downstream of PI3K to have enhancing role in regulation of the Raf/Erk signaling pathway downstream of Ras activated. PI3k inhibitor, LY294402 inhibited Erk activation by inhibiting Rac activation (Arai *et al.*, 2002). However, another downstream effector of PI3K may have a role in activation of Erk/Elk-1, further studies on signaling downstream of PI3K for regulation of EZH2 expression will be required to elucidate the molecular mechanisms.

EZH2 overexpression induced by the activated MEK–ERK1/2 pathway occurs in ERBB2-overexpressing and triple-negative breast cancer subtypes

We also explored the relevance of the signaling pathway that leads to EZH2 overexpression in breast cancer tissue. The result of immunohistochemical staining of the representative case with triple-negative breast cancer was shown in Figure 5. The cancer cells showed positivity for EGFR and pElk-1. The EZH2 that is supposed to be a downstream protein of MEK/ERK/Elk-1 pathway from the findings thus far demonstrated was overexpressed, and high MIB-1 index was also observed in the same area (Figures 5b–e). The two continuous and thin tissue sections showed the synchronized co-overexpression of EZH2 and pElk-1 proteins in individual cancer cells (Figures 5b and c). Among 178 breast cancer tissues, there was a significant correlation between EZH2 overexpression and breast cancer phenotype, the EZH2 protein expression positive rates of the ERBB2-overexpressing and triple-negative subtypes were much higher than that of the hormone receptor-positive subtype (Figure 6a). The percentages of cases classified as EZH2-overexpressing cases in the ERBB2-overexpressing subtype and triple-negative breast cancer subtype were much higher than in the hormone receptor-positive subtype (Figure 6b), suggesting that the MEK–ERK pathway mainly causes EZH2 overexpression in ERBB2-overexpressing and triple-negative breast cancer cells. In addition, the percentages of cases classified as RUNX3-negative or RUNX3-weakly expressed in cytoplasm in the triple-negative breast cancer subtype were much lower than in the hormone receptor-positive subtype (Figure 6c). We treated MDA-MB-231 cells with *Elk-1* siRNA transfection and examined whether the expression of *RUNX3* mRNA changed. As shown in Figure 6d, the expression of *RUNX3* mRNA started to increase 72 h after *Elk-1* knockdown.
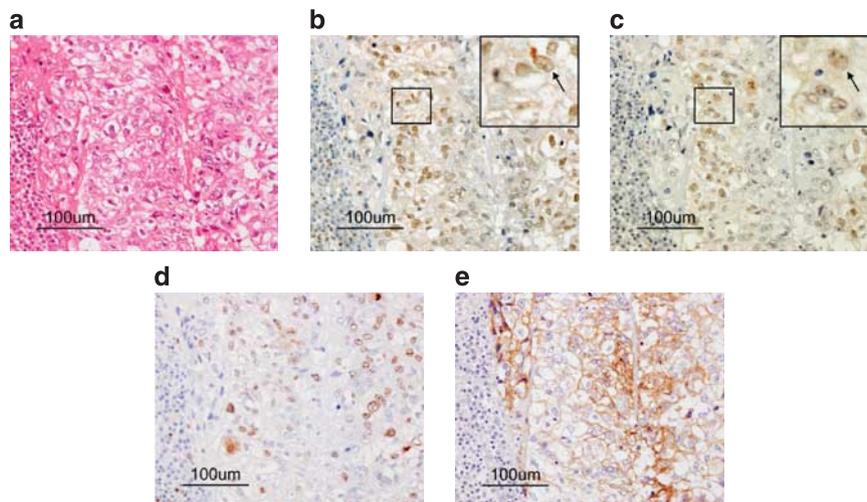

Figure 5 Immunohistochemical staining of breast cancer tissue of the triple- negative subtype. (**a**) H&E (hematoxylin and eosin), (**b**) EZH2, (**c**) pElk-1, (**d**) Ki-67 and (**e**) EGFR. Immunohistochemical stainings for EZH2 protein and pElk-1 protein were performed using the two continuous and thin tissue sections to show the positive correlation of expression of EZH2 protein and pElk-1 protein in individual cancer cells. The individual cancer cells surrounded by square box (marked by black arrow) were magnified to show the synchronized co-overexpression of EZH2 protein and pElk-1 protein.
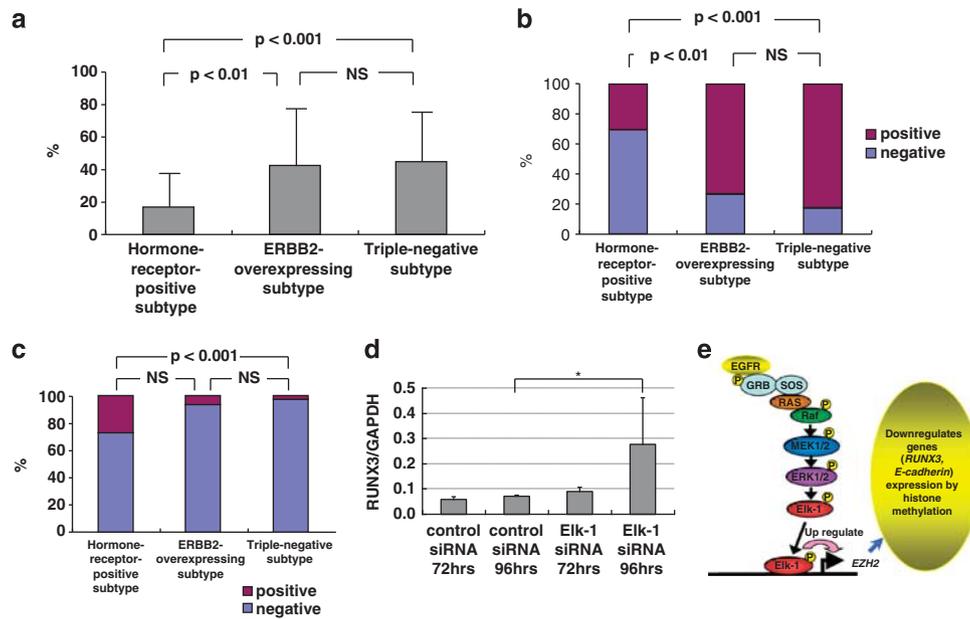
promoter was shown in this study, but the longer deletion variants of the constructed reporter plasmid exhibited relative low luciferase activity, suggesting that there may be binding sites for repressive transcriptional factors in those regions of the *EZH2* promoter. The plausible possibility that *EZH2* transcription is regulated by a variety of transcriptional factors would suggest that histone modification by a histone modifier protein such as EZH2 may be reversible in response to several factors in the microenvironment, including inflammation, hypoxia and carcinogen exposure around normal or cancer cells. Histone modifier proteins are capable of the transcription of a whole set of genes simultaneously. Further study will be needed to devise a methodology for cancer treatment by regulating the expression of histone modifier proteins.

Western blot analyses of ERBB2-positive and triple-negative breast cancer cell lines were carried out to explore the extent of the inhibitory effect of MEK inhibitor treatment or Elk-1 knockdown on EZH2 protein expression (Figure 4). The remarkable effect of the MEK inhibitor on EZH2 protein in triple-negative and ERBB2-overexpressing cells suggests that the MEK/ERK pathway activated via *KRAS* mutation, EGFR amplification and ERBB2 amplification contribute strongly to EZH2 overexpression. In fact, MDA-MB-231 and MDA-MB-468 cells are *KRAS* mutant and EGFR amplified breast cancer cells, respectively (Hollestelle *et al.*, 2010). Tissue microarray studies have shown a high rate of EGFR overexpression in triple-negative breast cancers (Cleator *et al.*, 2007). In this study, the EZH2 protein expression positive rates of the ERBB2-overexpressing and triple-negative subtypes were much higher than that of the hormone receptor-positive subtype (Figure 6a). On the basis of the results of this study, we think that EZH2 inhibition is a critical treatment in triple-negative and ERBB2-overexpressing breast cancer cells.

Many phenotypical and molecular features, including ER negativity, high nuclear grade, high Ki-67 staining, CK5/6 expression, EGFR expression and *p53* mutation, are shared by sporadic triple-negative breast cancers and tumors that arise in carriers of the *BRCA1* mutation (Crook *et al.*, 1998; Sørlie *et al.*, 2001; Foulkes *et al.*, 2004). *BRCA1* is rarely mutated in sporadic breast cancers (Futreal *et al.*, 1994), however, the histopathological similarity of the two categories; triple-negative breast cancers and tumors with the *BRCA1* mutation leads us to speculate that common pathways may be associated with cancer cell proliferation. Interestingly, a recent study immunohistochemically demonstrated a clear increase in EZH2 protein levels in tumors from *BRCA1* mutation carriers (Puppe *et al.*, 2009). It also showed that *BRCA1*-deficient cancer cells are selectively dependent on their elevated EZH2 levels and that inhibition of EZH2 is about 20-fold more effective in killing *BRCA1*-deficient cells than in killing *BRCA1*-proficient mammary tumor cells, suggesting that EZH2 may be a target for drug therapy of a specific subtype of breast cancer. The results of our present study suggest that inhibition of EZH2 may critically block cancer cell

proliferation in aggressive breast cancer phenotypes, including triple-negative breast cancers and BRCA1-deficient breast cancers.

The findings in this study showed that EZH2 overexpression was caused by activated MEK–ERK1/2-Elk-1 pathway. The signaling pathway connected to EZH2 overexpression is associated with aggressive phenotypes of breast cancer including triple-negative and ERBB2-overexpressing breast cancers. Our study could pave the way for EZH2 inhibition to become an efficient treatment for more aggressive breast cancers.

Materials and methods

Bioinformatic analysis and cloning of the EZH2 gene promoter region
By using the 5′ complementary DNA sequence of the *EZH2* gene as a probe, exons of the *EZH2* gene were identified as corresponding to the sequences of the nucleotides on human chromosome 7 (Gene Accession Number NC_000007. 12) by a BLAST search. The promoter and transcription binding sites on the 5′ flanking region of *EZH2* were predicted by conducting a TRANSFAC 6.0 analysis. The full-length *EZH2* gene promoter region from the 5′ flanking 2874-bp upstream region to 599-bp downstream region from the transcription starting site of the *EZH2* gene (148135408–148212347) was amplified by using human genomic placenta DNA (50 ng/µl) as a template and a PCR primer with an incorporated *Mlu*I site (EZH2−2874), and a primer with an incorporated *Bgl*II site (EZH2 + 599R) (Supplementary Table 1). The PCR product after digestion with *Bgl*II and *Mlu*I was inserted into the pGL3-Basic vector (Promega, Madison, WI, USA), and the entire length of the inserted PCR product was sequenced by using an ABI PRISM 3100 Genetic Analyzer (Applied Biosystems, Carlsbad, CA, USA) and the designed sequence primers (Supplementary Table 1).

Construction of recombinant luciferase reporter plasmids with the full-length EZH2 gene promoter region, deletion variants and mutation variant
The whole *Bgl*II–*Mlu*I fragment of the recombinant plasmid was subcloned into the *Bgl*II–*Mlu*I site of the MCS of the pGL3-Basic vector (Promega), and the plasmid obtained was designated as pGL3-2874. Several deletion variants designated as pGL3-2704, pGL3-2282, pGL3-2106, pGL3-1839, pGL3-1516, pGL3-1182, pGL3-1089, pGL3-696, pGL3-456, pGL3-151 and pGL3-9 were generated using primer sets of the forward primer with an incorporated *Mlu*I site or the reverse primer with an incorporated *Bgl*II site (Supplementary Table 1) as described above. The wild and mutant DNA sequences of the *EZH2* promoter region encompassing all the three Elk-1 binding sites (−453 nt to −180 nt) were synthesized, respectively and inserted into pGL3-Basic Vector. The wild-type and mutant-type constructs were designated as the pGL3–Elk-1–WT and pGL3–Elk-1–MT, respectively. T was replaced into A in each Elk-1 binding motif of pGL3–Elk-1–MT construct.

Cell culture and transfection of reporter plasmids
Human breast cancer cell line MDA-MB-231 was routinely grown in RPMI medium containing 10% fetal bovine serum and 10% glutamine. The reporter plasmids were transfected with Lipofectamine 2000 (Invitrogen, Camarillo, CA, USA).

Dual-luciferase reporter assay
Dual-luciferase reporter assays with the constructed reporter plasmids were carried out according to the manufacturer's

instructions (Promega). pRL-SV40 plasmid (Promega) was co-transfected to normalize the transfection efficiency. Transfections were carried out on 12-well plates, and the reporter assays were carried out on 96-well plates. Briefly, 4 h after transfection, the cell culture medium was replaced with fresh complete growth medium, and the cells were incubated for another 20 h. The activity of firefly (*Photinus pyralis*) and Renilla (*Renilla reniformi*) luciferases (luc+ and Rluc, respectively) in cell lysates was measured sequentially with a 96-well plate luminometer (Luminescencer-JNR AB-2100, Atto Bio-Instrument, Tokyo, Japan). Promoter strength was expressed as luc+ activity/Rluc activity.

Breast cancer cell lines
Three breast cancer cell lines, that is, MDA-MB-231, MDA-MB-468, SKBr3, and HCC1500, all obtained from the American Type Culture Collection (Manassas, VA, USA), were maintained at 37 °C in RPMI supplemented with 10% heat-inactivated fetal bovine serum and 1% glutamine under a 5% CO_2 atmosphere. MDA-MB-231 and MDA-MB-468 are basal-type breast cancer cell lines, which are defined by triple negativity for ER, PgR and ERBB2. SKBr3 cells are characterized by ERBB2 expression, HCC1500 cells are characterized by hormone-receptor expression (Hollestelle *et al.*, 2010).

RNA isolation and real-time RT–PCR
Total RNA from the cell lines was isolated with TRIzol Reagent (Invitrogen) and reverse transcribed to complementary DNA with ExScript RT Reagent (Takara, Yokkaichi, Mie, Japan). Real-time RT–PCR was carried out with specific primers for *EZH2* and *Elk-1* and a Smart Cycler (Cepheid, Sunnyvale, CA, USA). *GAPDH* expression was used to normalize for variance. Real-time fluorescence monitoring of the PCR products was performed with SYBR Green I fluorescent dye (Takara). The levels of expression of specific genes are reported as ratios to the level of expression of *GAPDH* in the same master reaction. The PCR primer pairs (5′ to 3′) used for each gene were: *EZH2*, CCCTGACCTCTG TCTTACTTGTGGA and ACGTCAGATGGTGCCAGCA ATA; *Elk-1*, CACTTCTGGAGCACCCTGAGTC and AGA GGCCATCCACGCTGATA; and *GAPDH*, GCACCGTCA AGGCTGAGAAC and ATGGTGGTGAAGACGCCAGT. These primer sets were designed by Takara.

MEK inhibitor, PI3K inhibitor and Akt inhibitor treatment
MDA-MB-231 cells were treated with a MEK inhibitor (U0126) (Promega) at a concentration of 40 μM for 4, 8, 12 and 24 h, and the other cell lines, including MDA-MB-468 and SKBr3 cells, were treated with the MEK inhibitor at 50 μM. MDA-MB-231 cells were treated with a PI3K inhibitor (LY294002) (Calbiochem, Darmstadt, Germany) or an Akt inhibitor (Akt inhibitor V, Triciribine) (Calbiochem) at a concentration of 1, 5, 10, 25, 50 μM for 24 h. Total RNA from the treated cell lines was then isolated and used for real-time RT–PCR for *EZH2*, *Elk-1* and *GAPDH*, ChIP assay and western blot analysis.

RNA interference
Two 21-nucleotide duplex siRNA for *Elk-1* and one negative control siRNA were synthesized by Ambion (Carlsbad, CA, USA), Inc. (*Elk-1* siRNA ID, s4634; *Elk-1* siRNA-1 and s4633; *Elk-1* siRNA-2), and 24 h after plating the cells they were transfected with *Elk-1* siRNA or control siRNA by using the DharmaFECT transfection reagent (Dharmacon, Lafayette, CO, USA) according to the manufacturer's instructions. Cells were harvested 48 h after transfection and subjected to several assays, including real-time RT–PCR, ChIP assay and western blot analysis.

Chromatin immunoprecipitation assay
The ChIP assay was carried out as previously described (Fujii *et al.*, 2003). The PCR conditions for the *EZH2* gene (Gene Accession Number NC_000007.12) promoter, which contains or does not contain Elk-1 biding motifs, were applied with the following three primer pairs: ChIP primer 1 which contains three Elk-1 binding motifs (5′ to 3′): TTAAAACCGTTACCA CCCCCGAGTTTTGAA and TTCGCTGTAAGGGACGCC ACTGGCCGTGT, ChIP primer 2 which contains two Elk-1 binding motifs (5′ to 3′): AACTCTGCGGCGCCGGTT CCCGCCAAGA and TTCGCTGTAAGGGACGCCACTG GCCGTGT and ChIP primer 3 which does not contain any Elk-1 binding motifs (5′ to 3′): ACGAACAGTGGA AGGGTCTG and GGAGTTTCGCTCTGGTTGTC. A ChIP primer pair for *GAPDH* as negative control for Elk-1 binding was used (5′ to 3′): CACCGTGTGCCCAAGACCTC and CAGCCCTGTAGCCTGGACCT (Morris *et al.*, 2005). A 5 μg amount of antibody was used in this assay. The antibodies used were phospho-Elk-1 and generic (pan-reactive) Elk-1 antibody purchased from Spring Bioscience (Pleasanton, CA, USA). Individual ChIP assays after treatment with the MEK inhibitor and *Elk-1* siRNA transfection were carried out at least three times to confirm the reproducibility of the PCR-based experiment. Preliminary PCR reactions were carried out to determine the optimal PCR conditions to assure linear amplification of the DNA. To measure the level of phospho-Elk-1 or generic Elk-1 binding in each immunoprecipitate, the ratios of immunoprecipitated DNA to input DNA were calculated by measuring the intensity of the PCR product in immunoprecipitated DNA versus input DNA (total chromatin) amplified by PCR in a linear range. The ratios were calculated using the PCR products by performing a DNA 1000 assay with the Agilent 2100 bioanalyzer and using DNA chips for electrophoresis (Agilent Technologies, Santa Clara, CA, USA).

Western blot analysis
Cells were lysed with whole-cell lysis buffer (80 mm glycerophosphate, 20 mm EGTA, 15 mm $MgCl_2$, 20 mm NAF, 150 mm NaCl, 1 mm EDTA, 0.5% NP-40, 10 mm Na_3VO_4, 1 mm phenylmethylsulfonyl fluoride and a protease inhibitor tablet (Roche, Mannheim, Germany), and the lysates were frozen in liquid nitrogen and thawed three times to rupture the cell membranes. Samples of the lysates were incubated for 30 min on ice to lyse the nuclei and then centrifuged at 8900 rpm. The protein concentration of each sample was determined with a BCA Protein Asssay Kit (Pierce, Rockford, IL, USA). Equal amounts of protein (20 μg) from each cell line were subjected to western blot analysis. The probing antibodies were EZH2 antibody (1:1000) (BD Transduction Laboratories, Sparks, MD, USA), phospho-p44/42 MAPK (ERK1/2) antibody (1:1000) (Cell Signaling Technology, Boston, MA, USA), p44/42 MAPK (ERK1/2) antibody (1:1000) (Cell Signaling Technology), phospho-Elk-1 antibody (1:200) (Santa Cruz, Santa Cruz, CA, USA), Elk-1 antibody (1:200) (Santa Cruz), Akt antibody (1:1000) (Cell Signaling Technology), pAkt antibody (Ser 473) (Cell Signaling Technology), and β-actin antibody (1:50) (Santa Cruz).

Breast cancer tissue samples
A total of 178 breast cancer specimens that had been histologically diagnosed as invasive ductal carcinoma were studied and classified into three types: a hormone receptor-positive type (ER- and/or PgR-positive), an ERBB2-

overexpressing type (ERBB2-overexpressing with/without hormone-receptor-positive) and triple-negative type (hormone receptor-negative and ERBB2 not overexpressed). All specimens were obtained from females (mean age 58.3 years; s.d. ± 11.1) by surgical resection at the National Cancer Hospital East, and the histological diagnosis was carried out by routine microscopic analysis of sections of formalin-fixed, paraffin-embedded specimens. None of the patients had received any preoperative treatment, including radiation therapy, hormone therapy or chemotherapy. A representative section that included the maximum diameter of the tumor was used for the immunohistochemical analysis. All clinicopathological data were according to the TNM classification (UICC) and obtained from the clinical and pathology records. Several clinicopathological factors were shown in Supplementary Table 2.

Immunohistochemical staining
The breast cancer tissues were used for the immunohistochemical analysis. Immunohistochemistry for EZH2 (1:25) (BD Transduction Laboratories), phospho-Elk-1 (1:25) (Spring Bioscience), MIB-1 (1:50) (Dako, Tokyo, Japan), EGFR (1:50) (Novocastra, New Castle, UK) and RUNX3 (1 µg/ml) (R3-6E9) (Ito *et al.*, 2005) was carried out on sections of formalin-fixed, paraffin-embedded tissue by microwave-induced epitope retrieval and with the Dako Envision detection system. Appropriate positive and negative internal controls were used to validate immunohistochemical staining.

Conflict of interest

The authors declare no conflict of interest.

References

Arai A, Kanda E, Miura O. (2002). Rac is activated by erythropoietin or interleukin-3 and is involved in activation of the Erk signaling pathway. *Oncogene* **21**: 2641–2651.

Bachmann IM, Halvorsen OJ, Collett K, Stefansson IM, Straume O, Haukaas SA et al. (2006). EZH2 expression is associated with high proliferation rate and aggressive tumor subgroups in cutaneous melanoma and cancers of the endometrium, prostate, and breast. *J Clin Oncol* **24**: 268–273.

Cao R, Wang L, Wang H, Xia L, Erdjument-Bromage H, Tempst P et al. (2002). Role of histone H3 lysine 27 methylation in Polycomb-group silencing. *Science* **298**: 1039–1043.

Cleator S, Heller W, Coombes RC. (2007). Triple-negative breast cancer: therapeutic options. *Lancet Oncol* **8**: 235–244.

Crook T, Brooks LA, Crossland S, Osin P, Barker KT, Waller J et al. (1998). p53 mutation with frequent novel condons but not a mutator phenotype in BRCA1- and BRCA2-associated breast tumours. *Oncogene* **17**: 1681–1689.

Foulkes WD, Brunet JS, Stefansson IM, Straume O, Chappuis PO, Bégin LR et al. (2004). The prognostic implication of the basal-like (cyclin E high/p27 low/p53+/glomeruloid-microvascular-proliferation+) phenotype of BRCA1-related breast cancer. *Cancer Res* **64**: 830–835.

Fujii S, Ito K, Ito Y, Ochiai A. (2008). Enhancer of zeste homologue 2 (EZH2) down-regulates RUNX3 by increasing histone H3 methylation. *J Biol Chem* **283**: 17324–17332.

Fujii S, Luo RZ, Yuan J, Kadota M, Oshimura M, Dent SR et al. (2003). Reactivation of the silenced and imprinted alleles of ARHI is associated with increased histone H3 acetylation and decreased histone H3 lysine 9 methylation. *Hum Mol Genet* **12**: 1791–1800.

Fujii S, Ochiai A. (2008). Enhancer of zeste homolog 2 downregulates E-cadherin by mediating histone H3 methylation in gastric cancer cells. *Cancer Sci* **99**: 738–746.

Futreal PA, Liu Q, Shattuck-Eidens D, Cochran C, Harshman K, Tavtigian S et al. (1994). BRCA1 mutations in primary breast and ovarian carcinomas. *Science* **266**: 120–122.

Gupta RA, Shah N, Wang KC, Kim J, Horlings HM, Wong DJ et al. (2010). Long non-coding RNA HOTAIR reprograms chromatin state to promote cancer metastasis. *Nature* **464**: 1071–1076.

Hollestelle A, Nagel JH, Smid M, Lam S, Elstrodt F, Wasielewski M et al. (2010). Distinct gene mutation profiles among luminal-type and basal-type breast cancer cell lines. *Breast Cancer Res Treat* **121**: 53–64.

Ito K, Liu Q, Salto-Tellez M, Yano T, Tada K, Ida H et al. (2005). RUNX3, a novel tumor suppressor, is frequently inactivated in gastric cancer by protein mislocalization. *Cancer Res* **65**: 7743–7750.

Kenny PA, Lee GY, Myers CA, Neve RM, Semeiks JR, Spellman PT et al. (2007). The morphologies of breast cancer cell lines in three-dimensional assays correlate with their profiles of gene expression. *Mol Oncol* **1**: 84–96.

Kleer CG, Cao Q, Varambally S, Shen R, Ota I, Tomlins SA et al. (2003). EZH2 is a marker of aggressive breast cancer and promotes neoplastic transformation of breast epithelial cells. *Proc Natl Acad Sci USA* **100**: 11606–11611.

Konecny G, Pauletti G, Pegram M, Untch M, Dandekar S, Aguilar Z et al. (2003). Quantitative association between HER-2/neu and steroid hormone receptors in hormone receptor-positive primary breast cancer. *J Natl Cancer Inst* **95**: 142–153.

Korsching E, Jeffrey SS, Meinerz W, Decker T, Boecker W, Buerger H. (2008). Basal carcinoma of the breast revisited: an old entity with new interpretations. *J Clin Pathol* **61**: 553–560.

Morris DP, Michelotti GA, Schwinn DA. (2005). Evidence that phosphorylation of the RNA polymerase II carboxyl-terminal repeats is similar in yeast humans. *J Biol Chem* **280**: 31368–31377.

Nielsen TO, Hsu FD, Jensen K, Cheang M, Karaca G, Hu Z et al. (2004). Immunohistochemical and clinical characterization of the basal-like subtype of invasive breast carcinoma. *Clin Cancer Res* **10**: 5367–5374.

Perou CM, Sørlie T, Eisen MB, van de Rijn M, Jeffrey SS, Rees CA et al. (2000). Molecular portraits of human breast tumours. *Nature* **406**: 747–752.

Plath K, Fang J, Mlynarczyk-Evans SK, Cao R, Worringer KA, Wang H et al. (2003). Role of histone H3 lysine 27 methylation in X inactivation. *Science* **300**: 131–135.

Puppe J, Drost R, Liu X, Joosse SA, Evers B, Cornelissen-Steijger P et al. (2009). BRCA1-deficient mammary tumor cells are dependent on EZH2 expression and sensitive to Polycomb Repressive Complex 2-inhibitor 3-deazaneplanocin A. *Breast Cancer Res* **11**: R63.

Raaphorst FM, van Kemenade FJ, Blokzijl T, Fieret E, Hamer KM, Satijn DP *et al*. (2000). Coexpression of BMI-1 and EZH2 polycomb group genes in Reed-Sternberg cells of Hodgkin′s disease. *Am J Pathol* **157**: 709–715.

Schuettengruber B, Chourrout D, Vervoort M, Leblanc B, Cavalli G. (2007). Genome regulation by polycomb and trithorax proteins. *Cell* **128**: 735–745.

Slamon DJ, Godolphin W, Jones LA, Holt JA, Wong SG, Keith DE *et al*. (1989). Studies of the HER-2/neu proto-oncogene in human breast and ovarian cancer. *Science* **244**: 707–712.

Sørlie T, Perou CM, Tibshirani R, Aas T, Geisler S, Johnsen H *et al*. (2001). Gene expression patterns of breast carcinomas distinguish tumor subclasses with clinical implications. *Proc Natl Acad Sci USA* **98**: 10869–10874.

Varambally S, Cao Q, Mani RS, Shankar S, Wang X, Ateeq B *et al*. (2008). Genomic loss of microRNA-101 leads to overexpression of histone methyltransferase EZH2 in cancer. *Science* **322**: 1695–1699.

Varambally S, Dhanasekaran SM, Zhou M, Barrette TR, Kumar-Sinha C, Sanda MG *et al*. (2002). The polycomb group protein EZH2 is involved in progression of prostate cancer. *Nature* **419**: 624–629.

Supplementary Information accompanies the paper on the Oncogene website (http://www.nature.com/onc)